Appl Biochem Biotechnol
DOI 10.1007/s12010-015-1906-6

Cloning, Expression, Mutagenesis Library Construction of Glycerol Dehydratase, and Binding Mode Simulation of Its Reactivase with Ligands

Wei Jiang[1,2] · **Wenjun Li**[3] · **Yan Hong**[4] · **Shizhen Wang**[1,2] · **Baishan Fang**[1,2,5]

Received: 8 September 2015 / Accepted: 21 October 2015

Abstract The production of 1, 3-propanediol (1, 3-PD) and 3-hydroxypropionaldehyde (3-HPA) by enzyme reaction has been a hot field, and glycerol dehydratase (GDHt) is the key and rate-limiting enzyme involved in their biosynthesis. The *gld*ABC gene encoding GDHt was cloned from *Klebsiella pneumoniae*, and the activity of the corresponding proteins expressed extracellularly and intracellularly was 6.8 and 3.2 U/mg, respectively, about six and three times higher than that of the wild strain. The change of amino acids for the β subunit can adjust the length of the Co–N bond and affect the homolysis rate of the Co–C bond to change GDHt activity. The expression plasmid, pET-32a-*gld*AC (containing no *gld*B which encodes the β subunit of GDHt), was constructed to build the mutagenesis library to improve the GDHt activity. The binding models of glycerol dehydratase reactivation factor (GDHtR) with ATP, CTP, or GTP were simulated by semi-flexible docking, respectively, and there was almost no difference between them. This research provided the basis for studying the quantitative

Highlights • The specific activities of pET-32a-*gld*ABC and pET-22b-*gld*ABC were six and three times those of the wild type.
• An expression plasmid without *gld*B was built to construct a mutagenesis library.
• The binding modes of the GDHtR with ATP, CTP, or GTP, respectively, were simulated.
• The binding modes were almost no different basis for finding out inexpensive ligands to replace ATP.

✉ Baishan Fang
fbs@xmu.edu.cn

[1] Department of Chemical and Biochemical Engineering, College of Chemistry and Chemical Engineering, Xiamen University, Xiamen 361005, China

[2] The Key Lab for Synthetic Biotechnology of Xiamen City, Xiamen University, Xiamen 361005, China

[3] Hangzhou DAC Biotech Co., Ltd, Hangzhou 310000, China

[4] Jingdezhen Ceramic Institute of Materials Science and Engineering, Jingde Zhen 333000, China

[5] The Key Laboratory for Chemical Biology of Fujian Province, Xiamen University, Xiamen, Fujian 361005, China

Published online: 07 November 2015

structure-activity relationships between GDHtR and its ligands, as well as searching inexpensive ligands to replace ATP. These results and methods are of great use in economical and highly efficient production of 3-HPA and 1, 3-PD by the enzyme method.

Keywords GHDt · Cellular and extracellular expression · GHDtR · Molecular chaperone · Molecular DOCK

Introduction

Glycerol dehydratase (EC 4.2.1.30, GDHt) is a key and rate-limiting enzyme in the bioconversion process of glycerol to 3-hydroxypropionaldehyde (3-HPA), which is further reduced to 1, 3-propanediol (1, 3-PD) by 1, 3-propanediol dehydrogenase (PDOR). 3-HPA is an important chemical industry material, being a potent bacterial inhibitor and precursor in the production of numerous industrial chemicals, such as 1, 3-PD [1, 2]. 1, 3-PD, as a bifunctional organic compound and a key component of the emerging polymer business, has numerous applications in polymers, medicines, foods, cosmetics, and lubricants [2, 3]. It has been done to improve the enzymatic production of 1, 3-PD by enzymatic reaction due to its decisive industrial value.

Enhancing the expression level and activity of GDHt will be essential for the production 1, 3-PD, as its rate-limiting effect. While most researchers have been focusing on productivity and optimum conversion conditions of wild forms of GDHt [1, 3], it is necessary to analyze the expression methods, improve enzyme activity, and explore the GDHt enzymatic properties as well as the reactivating mechanism. The coenzyme B_{12}-dependent GDHt consists of three homodimers in the form of $\alpha_2\beta_2\gamma_2$ and has a typical $(\beta/\alpha)_8$ barrel in its α-subunit forming the active site [4, 5]. Researchers have focused on *Klebsiella pneumoniae*, *Citrobacter freundii*, and *Clostridium butyricum* more than others due to their high conversion and strong productivity of 1, 3-PD. Protein engineers redesigned proteins to increase their biomedical or industrial utility [6]. Despite the reported crystal structures of B_{12}-dependent GDHt [4, 5] as well as the enhanced pH stability and activity of GDHt from *K. pneumoniae* [7, 8], little has been done concerning their structure-activity relationships and no report about the directed evolution treatment on the GDHt has been found.

The coenzyme B_{12}-dependent rearrangement and dehydration of glycerol to 3-HPA are catalyzed by GDHt, which undergoes mechanism-based inactivation by glycerol or oxygen during the catalytic process. The fine mechanism of coenzyme B_{12}-dependent diol dehydratase (DDH) and the energetic feasibility of enzymatic radical catalysis were described [9]. It was demonstrated that the glycerol dehydratase reactivating factor (GDHtR) is a molecular chaperone which participates in reactivation of the inactivated enzymes [10]. Currently, GDHt reactivase apparently attracts the attention of more researchers to overcome this. In the presence of ATP, Mg^{2+}, coenzyme B_{12}, and GDHtR, the inactivated GDHt could be rapidly reactivated by exchanging the modified coenzyme with intact coenzyme B_{12} [11, 12]. Research showed that the catalytic efficiency of the deactivated GDHt, which was resurrected by ATP, has no obvious decrease, and it still can maintain its high activity in the whole process of fermentation with enough energy and coenzyme [13, 14]. A study about the activity of GDHtR from *K. pneumoniae* has been reported [15].

Owing to GDHtR's extremely low ATP-hydrolyzing activity, it was defined as a molecular chaperone [16]. GDHtR mediates ATP-dependent reactivation by completely substituting the

enzyme-bound cobalamin lacking adenosine with intact adenosylcobalamin resulting in intermediary formation of apoenzyme [17]. The DOCK, the primary molecular docking software developed by Kuntz and his colleagues (http://dock.compbio.ucsf.edu/DOCK_6/dock6_manual.htm#TableofContents) [18], can automatically simulate the interactive model of ligands in the receptor activity sites, and predict and note the best interaction theory. Molecular dynamics (MD) simulations can reveal the microscopic nature of intermolecular interactions. Thus, the method has been successfully used in various fields [19–28]. The method also can automatically search the three-dimensional structure of the ligand from the database, so it is widely used in drug design. In drug design, the lead candidates can be found by using the docking algorithm that tries to identify the optimal binding mode of a small molecule (ligand) to the active site of a macromolecular target. The mechanism by which docking fidelity is achieved for the multitude of cofactor-dependent enzymes is poorly understood [29]. Herein the *gld*ABC gene encoding GDHt was cloned from *K. pneumoniae*, and expressed in *Escherichia coli* BL21 (DE3) pLysS by cellular and extracellular expression vectors, respectively. Besides that, the mutagenesis library of the *gld*B, which encodes the β-subunit of the GDHt, was constructed. In order to reveal the binding modes of the GDHtR with its molecular chaperone, the semi-flexible docking method was introduced in this study.

Materials and Methods

Strains, Plasmids, and Reagents

The strain *K. pneumoniae* DSM2026 was obtained from Doctor An-Ping Zeng (German Research Center for Biotechnology). *E. coli* DH5α and *E. coli* BL21 (DE3) pLysS were used as host strains for gene cloning and protein expression, respectively. And the expression plasmids, pET-22b (+) and pET-32a (+), were also used for expression of the *gld*ABC gene in different host strains.

All the enzymes for use in the study, such as restriction endonucleases, T4 DNA ligase, and Ex *Taq*™ DNA, were purchased from TaKaRa except RNase A which was from AMRESCO (Xiamen, China). The Agarose Gel DNA Fragment Recovery Kit Ver.2.0 and pMD18-T were obtained from TaKaRa and GeneRuler™ Ladder Mix from MBI Co. All the chemicals used were analytically graded and purchased from both Sigma and Omiga.

Gene Cloning and Recombinant Plasmid Construction

The targeted gene, *gld*ABC, was cloned based on the polymerase reaction (PCR) with the forward primer G1 (5′-CGGAATTCGTCTGAGGATTTCACCTTTTG-3′; the *Eco*RI restriction site is underlined) and the reverse primer G2 (5′-GCGAAGCTTGCTTCCTTTACGCAGCTTATG-3′; the *Hin*dIII restriction site is underlined) by the following temperature program: denaturation at 95 °C for 5 min and 30 cycles of 50 s at 95 °C, 1 min at 56 °C, and 3 min at 72 °C, followed by a 10-min extension at 72 °C. After double digested with *Eco*RI and *Hin*dIII, the resulting PCR product was gel purified and cloned into the *Eco*RI-*Hin*dIII sites of pET-22b (+) (extracellular expression vector) and pET-32a (+) (cellular expression vector), generating pET-22b-*gld*ABC and pET-32a-*gld*ABC, respectively. Then, the recombinant plasmids were transformed into competent *E. coli*

DH5α and sequence after cultivation at 37 °C. Then, the positive one was transformed into *E. coli* BL21 (DE3) pLysS for protein expression.

Expression of Recombinant Enzyme and Enzyme Assay

DE3 strains harboring the recombinant plasmid were incubated into LB liquid medium containing ampicillin (75 μg/mL) and incubated at 37 °C overnight. Subsequently, the mixture was transferred to fresh LB liquid medium (1:100 dilution) containing ampicillin (75 μg/mL) and cultured at 37 °C for 2 h. At an optical density (OD_{600}) of 0.5–0.6, isopropyl-β-D-thiogalactopyranoside (IPTG) was added to a final concentration of 1 mM, and the mixture was incubated at 37 °C for 5 h. Then, the cells were harvested for enzyme assay. Cell-free extract was obtained by the following steps: the induced restructuring cell was subjected to centrifugation for 10 min at 1 °C, 6500*g*/min, to remove the supernatant. Then, the buffer was added in the ratio between the cultures and binding buffer of 100:4, the cells were suspended, and the lysozyme added (final concentration 1 mg/mL); the mixture was placed in an ice bath for 30 min, incubated at 4 °C for 10 min, and finally centrifuged for 10 min at 4 °C and 13,000*g*/min; and the supernatant was collected, which was a cell-free extraction liquid (or thick enzyme fluid). After that, the GDHt enzyme activity and protein concentration were detected before assaying the specific activity of the GDHt. The binding buffer (pH 7.8) was prepared with 0.2 mol/L sodium phosphate and 0.5 mol/L NaCl.

The GDHt activity was measured with 1, 2-PD as substrate as previously described by Daniel et al. [30], with moderate modifications. One unit (U) of enzyme activity was defined as the amount of the enzyme consumed in catalyzing 1.0 μmol substrate per minute. Specific activity, which was defined as the ratio of enzyme activity (U/mL) to protein concentration (mg/mL), was expressed as units/milligram protein.

Mutagenesis Library of the *gld*B

The *gld*A (encoding α subunit) was cloned by PCR with the forward primer G1 (5′-CGGAATTCGTCTGAGGATTTCACCTTTTG-3′; the *Eco*RI restriction site is underlined) and the reverse primer A2 (5′-GCGAGCTCTTATTCAATGGTGTCGG-3′; the *Sac*I restriction site is underlined). After being double digested with *Eco*RI and *Sac*I, the PCR product was gel purified and cloned into the *Eco*RI-*Sac*I sites of pET-32a (+), generating pET-32a-*gld*A. The *gld*C (encoding γ subunit) was cloned by PCR with the forward primer C1 (5′-CGTCGACGGGAGTGACCATGAGC-3′; the *Sal*I restriction site is underlined) and the reverse primer G2 (5′-GCGAAGCTTGCTTCCTTTACGCAGCTTATG-3′; the *Hin*dIII restriction site is underlined). After being double-digested with *Sal*I and *Hin*dIII, the PCR product was gel-purified and cloned into the *Sal*I-*Hin*dIII sites of the pET-32a-*gld*A, generating pET-32a-*gld*AC without *gld*B (encoding β subunit). The mutagenesis *gld*B obtained by error-prone PCR could be tandem expression of the *gld*A and *gld*C due to the introduction of *Sac*I and *Sal*I restriction sites between the *gld*A and *gld*C.

Semi-flexible Docking

Based on the crystal structure information of the GDHtR (PDB, ID: 1NBW), semi-flexible docking method was applied to simulate the binding modes of GDHtR with ATP, CTP, or GTP, respectively, and their binding free energy, van der Waals force, and electrostatic force were

calculated in the following six steps: (i) prepare receptor files: open 1NBW.pdb in the Chimera; delete B, C, and D subunits and water molecules, and only retain A subunit; complement parameter of receptors using the Dock Prep tool; add hydrogenation and charge for the receptor; and then save as mol2 format; (ii) prepare ligand file: draw molecular formulas of ATP, CTP, and GTP by Chemoffice; generate three molecular structural formulae using Chem3D Ultra 10.0; add hydrogenation and charge for the ligands (charge type Gasteiger-Hückel); and then save as mol2 format; (iii) generate the target protein molecular surface: set parameters and run the DMS program-generated receptor solvent polarization surface; the cygwin users need to use the vi. command processing; the generated molecular surface is used to calculate each negative mold ball size; (iv) generate the negative mode: the receptor molecules are larger in this work, and there is a need to abridge the receptor molecules with the Chimera program; retain ATPase domain structure, and then use sphgen program in the DOCK 6.0 generated spherical negative mode which is required for docking; choose one of the biggest negative of modulis; and use the DOCK 6.0 showsphere procedure observation the negative mode; (v) the generated grid: set the position and size of the box around the active site using showbox program to generate a box used to compute the grid; compile the grid parameter file and run the grid application to calculate box of electrostatic interactions, and van der Waals interaction energy within the grid file; the generated ratings of the grid were saved in *.cnt, *.nrg, and *.bmp files; (vi) flexible ligand molecular docking: compile the flexible docking parameters in the dock.in file, run DOCK 6.0 procedures, and complete the docking. Search the lowest energy structure.

Results and Discussion

Gene Cloning and Sequence Analysis

The *gld*ABC gene was 2735 bp, and the α, β, and γ subunit genes were 1668, 585, and 426 bp, respectively. The gene length of the three subunits was the same as that of the previous report [31].

Recombinant Plasmid Construction and Enzyme Assay

In the study, the *E. coli* BL21 (DE3) pLysS was selected as the expression host due to the following reasons: firstly, the *E. coli* BL21 (DE3) pLysS was much more compatible with chloramphenicol resistance expression than *E. coli* BL21 (DE3), and it encoded a small amount of T7 lysozyme (T7 RNA polymerase natural inhibitor) plasmids which can guarantee stability of the target gene; secondly, pLysS has little effect on cell growth, and its tolerance toward the carrier of genetic toxicity was improved; thirdly, the preparation of cell extract was particularly convenient with pLysS as the expression host: after protein expression, collect cells, add 50 L Tris-HCl and 2 mmol/L EDTA pH 8.0 buffer, then simple freeze thawing or add 0.1 % TritonX-00, finally the intracellular T7 lysozyme can be effectively cracking cells [32].

In the intracellular expression, the GDHt activity cannot be detected through a simple method such as the host growth or no growth, medium color change and the emergence of a particular reaction, etc. to screen the purpose gene. Since GDHt enzyme activity was detected by the color of aldehyde which was produced by the reaction of cell extract and substrate, it gives many difficulties for the screening work of the molecular-directed evolution of GDHt.

But the extracellular expression GDHt can overcome this difficulty as it provides another way of screening which was a key limit point of directed evolution. The GDHt extracellular expression plasmid was constructed to fundamentally reduce the screening work and develop a more intuitive and simple screening method, such as sensitivity to the substrate glycerol, dependence on vitamin B_{12}, etc.

The engineering bacteria containing the expression vector pET-32a-*gld*ABC was induced for expression with 1.0 mM inducer IPTG concentration at 37 °C for 4 h. The vitality and specific activity of the pET-32a-*gld*ABC/BL21 (DE3)pLysS were 0.476 U/mL and 6.8 U/mg, respectively. With 1.0 mM inducer IPTG concentration at 25 °C for 5 h, the engineering bacteria containing expression vector pET-22b-*gld*ABC were induced for expression. The intracellular GDHt activity and specific activity of the pET-22b-*gld*ABC/BL21(DE3)pLysS were 0.224 U/mL and 3.2 U/mg, respectively. The value 0.224 U/mL displayed little difference with the interstitial cell activity (0.196 U/mL), suggesting that the recombination GDHt had been secreted into the periplasmic space of cells and had a small leakage into the medium. It was demonstrated that induced delay (16 h or overnight) could promote fusion protein leakage into the medium when the fusion proteins were transported to the periplasm [32].

The Activity Curve of the GDHt with Glycerol and 1, 2-PD as the Substrate

As aldehyde content should be in a straight line up when 1, 2-PD was used as substrate [30, 33], aldehyde content was detected in the GDHt reaction system only in 0.2 mol/L 1, 2-PD at the first 1 and 10 min, and the result is shown in Fig. 1. The aldehyde content of the GDHt reaction system was measured in 0.5, 1, 2, 4, 6, 8, and 10 min with 0.2 mol/L glycerol as substrate. It could be found that the absorbance values in 2~10 min rise significantly slowly at 305 nm, which means that the GDHt activity is quickly disappearing and the substrate glycerol resulted in the deactivation of GDHt. However, the GDHt activity could be stable before the first 1 min (Fig. 1), and the result was the same as previously reported [34], showing that the substrate glycerol inactivates GDHt easily.

The G/P $\text{ratio}_{1\ \text{min}}$ was described as the ratio of the GDHt activity with glycerol as substrate to the GDHt activity with 1, 2-PD as substrate after 1 min of reacting time. G/P $\text{ratio}_{1\ \text{min}}$=2.45

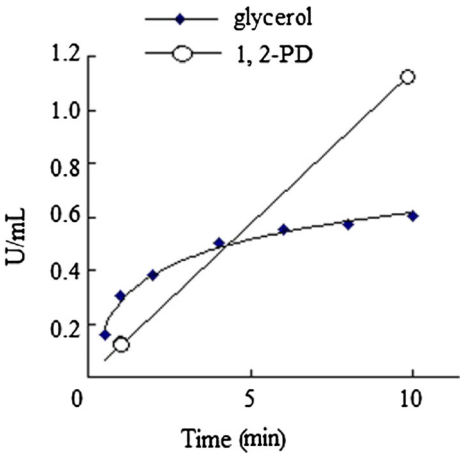

Fig. 1 Activity of the GDHt expressed by plasmid pET-32a-*gld*ABC using glycerol and 1, 2-PD as substrate

means that the GDHt had higher energy when the glycerol was used as substrate, and *G*/*P* ratio$_{10\ min}$=0.53 means that the GDHt activity with 1, 2-PD as substrate was nearly one times higher than that with glycerol as substrate when the reaction time was extended to 10 min, suggesting that glycerol can cause GDHt irreversible inactivation in a short time; thus, the GDHt activity can be detected by using 1, 2-PD as the substrate.

Mutagenesis Library of the *gld*B

With *Sac*I and *Sal*I restriction sites between the *gld*A and *gld*C, the mutagenesis *gld*B which was produced by error-prone PCR could be co-expressed along with the *gld*A and *gld*C. From the crystal structure of the GDHt, it can be seen that the α and β subunits were combined with vitamin B_{12}, and deoxidization acyl groups of vitamin B_{12} toward α subunit while β subunits mainly combine with the DBI (5, 6-dimethylbenzimidazole) of coenzyme. That is to say, the α and β subunits were located in different sides of the corrin ring, and the former center provides the adenosine free radicals of vitamin B_{12} on the catalytic substrate dehydration while the latter fix the coenzyme spatial location mainly through combination to the other side of the coenzyme DBI tail. However, different angles and bond length of the Co–N bond would influence the way of fracture of the Co–C bond [35]. In fact, the stretching of the Co–N bond would be done while the Co–C bond prefers to crack and generate acyl nucleoside free radicals with catalytic activity [36]. From the crystal structure of the GDHt and the DDH [4, 37], it could be found that the length of the GDHt Co–N bond was longer than that of the DDH, possibly explaining why the Michaelis constant *K*m of DDH for vitamin B_{12} was nearly 100 times that of GDHt (Table 1). So there is reason to believe that the change of the amino acids for the β subunit was to adjust the length of the Co–N bond affecting the homolysis rate of the Co–C bond to improve the GDHt activity. And a variety of information showed that the β subunit has a lot to do with the release of free radicals after the GDHt combination with the coenzyme [4, 37]. While bioinformatics software cannot accurately predict beneficial mutations, the best approach for directed evolution for the β subunit is error-prone PCR. For the β subunit, active sites were very scattered and *gld*B gene is only about 600 bp, meeting the optimum conditions of error-prone PCR amplification.

It could be seen from Table 1 that the Co–N key in the GDHt was longer than the Co–N key in the DDH, long on the affinity of vitamin B_{12} for the GDHt. And the DDH experiment found that the GDHt Michaelis constant of vitamin B_{12} of *K*m is nearly 100 times less than the vitamin B_{12} DDH Michaelis constant of *K*m .

Table 1 Distance of the Co–N bond in DDH, GDHt, and CN-cbl

Enzyme	Co-N Dis (100 K)	Ref.
DDH	2.5 Å	[37]
GDH	2.6 Å	[4, 16]
CN-cbl	2.18 Å	[37]

Directed evolution could overcome the limitations of natural enzymes, for it does not base on the detailed understanding of the structure-function relationship, but the simple powerful Darwinian principles of mutation and selection [38]. The GDHt extracellular expression plasmid was constructed for highly effective screening and significantly reducing the workload.

Semi-flexible Docking

Confirmation of Active Site for GDHtR

Using sphgen program, the biggest negative mold in ATPase structure domain (the location of the biggest negative mold could be the combined location ligands) is shown in yellow ball negative mold in Fig. 2, and it was to further confirm whether the negative mold was the combination location for ATP, CTP, or GTP, by comparison to the crystalline structure (PDB ID 2 d0o) of DDH reactivase which combines with the ADP.

Semi-flexible Docking of the GDHtR and ATP

The bonding model of the GDHtR and ATP after docking is shown in Fig. 3a, and the ATP occupied the active site of the GDHtR. The structural delineation of the ATP-binding site would be contributing to stimulate development of new pharmacological agents [39]. In the complexes of the GDHtR and the ATP, residues Asp8 (side chain carboxyl), Asn11 (side chain carbonyl), Gly419 (main chain amide group), Lys40 (side chain amide group), Gly80 (main chain carbonyl), Asp415 (side chain carboxyl), Ala418 (main chain amide group), and Asn442 (side chain amide group) of the GDHtR bound with ATP, respectively, generating nine additional hydrogen bonds (Fig. 3b).

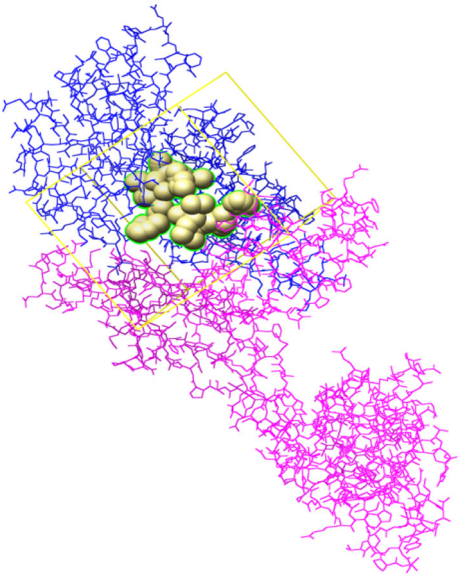

Fig. 2 Confirmation of the active site for the GDHtR. The ATPase domain is shown in *blue*; the insert domain, swiveling domain, and link domain are shown in *pink*; the active site is shown as *balls* in *yellow*; the *grid box* is shown in *yellow*

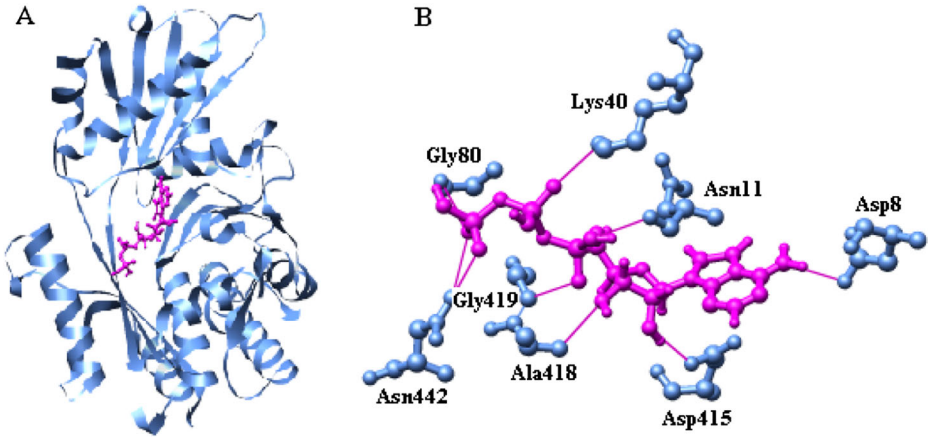

Fig. 3 Semi-flexible docking of the GDHtR and ATP. **a** The binding modes; **b** nine H-bonds between ATP and *Asp8*, *Asn11*, *Gly419*, *Lys40*, *Gly80*, *Asp415*, *Ala418*, and *Asn442*

Semi-flexible Docking of the GDHtR and CTP

The binding model of the GDHtR and CTP, which exhibited a slight difference with that of ATP, is shown in Fig. 4a after docking, and the CTP occupied the active site of the GDHtR. In the complexes of the CTP and the GDHtR, residues Asp8 (side chain carboxyl), Asn11 amide (main chain amide group), Lys40 (side chain amide group), Val78 (main chain carbonyl), Ala418 amide (main chain amide group), Gly419 amide (main chain amide group), Asp422 (side chain carboxyl), and Ala595 (main chain amide group) of the GDHtR bound with CTP, respectively, generating nine hydrogen bonds (Fig. 4b).

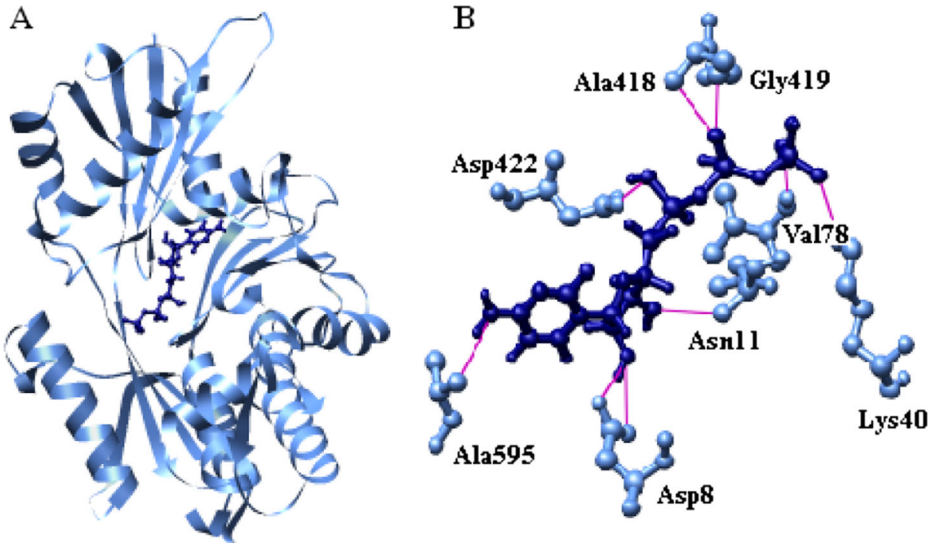

Fig. 4 Semi-flexible docking of the GDHtR and CTP. **a** The binding modes; **b** nine H-bonds between CTP and *Asp8*, *Asn11*, *Lys40*, *Val78*, *Ala418*, *Gly419*, *Asp422*, and *Ala595*

Semi-flexible Docking of the GDHtR and GTP

The binding mode, which was made through GDHtR and GTP docking, is shown in Fig. 5a. The GTP occupied the active site of the GDHtR and the combination pattern was similar to that of the CTP. Residues Asn11 (side chain amide group and main chain carbonyl), Lys40 (side chain amide group), Gly80 (main chain amide group), Glu393 (side chain carboxyl), Ala418 (main chain amide group), Asp422 (side chain carboxyl), and Ala595 (main chain amide group a) of the GDHtR bound with the GTP in the binding mode, respectively, generating eight additional hydrogen bonds (Fig. 5b).

The Binding Energy

The energetics of the ligand in a complex with the receptor, which was calculated by the DOCK6.0, is shown in Table 2. No significant difference was observed in the values of the binding free energy (grid score), van der Waals force (Vdw score), and electrostatic force (Es score) of GDHtR combining with the ATP, CTP, and GTP while the value of GTP was a little lower than the others. In addition, the van der Waals force plays more effect on the binding free energy contribution than the electrostatic effect.

In the process of ATP to ADP in the catalytic hydrolysis of the GDHtR, the GDHtR structure changed and was stimulated to combine with the deactivated GDHt, which prompted the damaged coenzyme B_{12} to dissociate from the GDHt activity center [10]. Hitherto, no report has been discovered about the binding mode of the GDHtR and ATP. Using DOCK6.0 software, the combination modes and the interaction between the GDHtR and ATP, CTP, or GTP were simulated through molecular semi-flexible docking. From the results, it can be seen that there was almost no difference between the combination modes and the interaction of the GDHtR and ATP, CTP, or GTP: (i) the number of hydrogen bonds were nine, nine, and eight, respectively; (ii) the binding energy, van der Waals, and electrostatic effect in the ligand were also relatively similar; and (iii) the van der Waals force affect the binding energy contribution more than other. Simulation results and experimental results are identical with each other. It

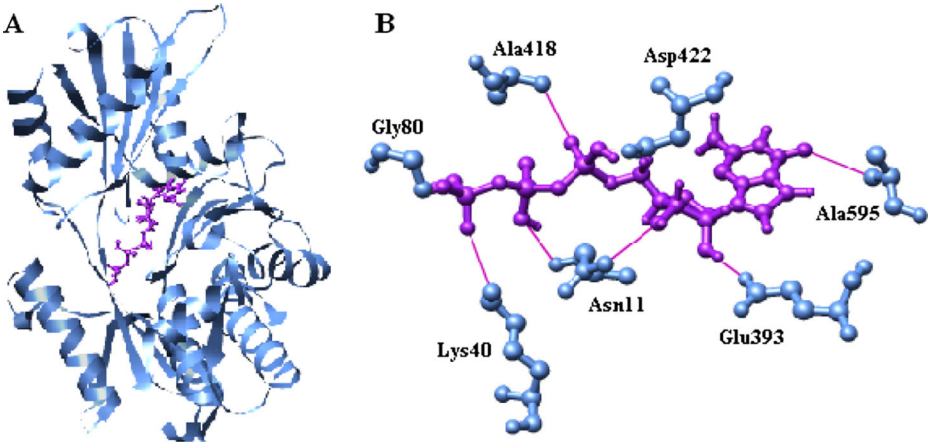

Fig. 5 Semi-flexible docking of the GDHtR and GTP. **a** The binding modes; **b** eight H-bonds between GTP and *Asn11*, *Lys40*, *Gly80*, *Glu393*, *Ala418*, *Asp422*, and *Ala595*

Table 2 The energetics of the ligand in complex with the receptor

Components	ATP	CTP	GTP
Grid score (kcal/mol)	−74.082	−75.311	−82.145
Vdw score (kcal/mol)	−53.552	−55.667	−60.018
Es score (kcal/mol)	−20.530	−19.6434	−22.127

has already been confirmed that CTP and GTP were able to replace ATP partially in the in situ reactivation of the glycerol-inactivated glycerol dehydratase [40]. And similar results were found by Motoyuki Hattori and Eric Gouaux in which CTP and ATP contain similar "amidine" functional groups within their base ring structures, and the CTP can bind to and activate P2X receptors like ATP [39]. The similarity of these combination modes demonstrated that CTP or GTP could supersede ATP to act as a distinct role in the GDHtR active center.

Drugs are typically discovered by chance in a trial-and-error manner using high-throughput screening methods which were used in in vitro experiments to assay the activity of a large number of compounds against a given target [41]. The process is expected to be very costly and time-consuming. If the 3D structure of the target is known, then simulated molecular docking can serve as a useful tool in the drug-discovery process [41]. The process of the GDHt reactivation required ATP, Mg^{2+}, coenzyme B_{12}, and the GDHtR, and the cost would be great to the industry if the ATP was used in this road. In this work, the binding models of GDHtR, with ATP, CTP, or GTP, respectively, were simulated by semi-flexible docking and their binding free energy, van der Waals force, and electrostatic force were calculated. This would be the basis for establishing quantitative structure-activity relationships of GDHtR and its ligands. According to the quantitative three-dimensional structure-activity relationship, using molecular docking means such as DOCK to analog filter the ATPase activity domain of the GDHtR from a small-molecule database such as ZINC aims at obtaining some cheap small-molecule ligand material to replace the ATP in the production process.

ATP, best known for its roles in studying the methylmalonic aciduria [29], immunogenic cancer cell death (immunogenic apoptosis) [42, 43], plant stress resistance [44], energy metabolism, intracellular signaling, biosynthetic reactions and active transport, et al., is a crucial extracellular signaling molecule [39]. Macromolecular assemblies that regulate chromatin structure using the energy of ATP hydrolysis have critical roles in development, cancer, and stem cell biology [45]. The simulation of the binding sites, combination model and binding energy of ATP with enzyme, and the substitution of ATP would help in promoting the development of related research.

Conclusions

In summary, the *gld*ABC gene encoding GDHt was cloned from *K. pneumoniae* DSM2026. The enzymes of pET-32a-*gld*ABC (for cellular expression) and pET-22b-*gld*ABC (for extracellular expression) had been examined to be 6.8 and 3.2 U/mg, about six and three times that of the wild type, respectively. The empty expression plasmid pET-32a-*gld*AC containing no *gld*B was under construction to ligate a mutagenesis fragment of the *gld*B to construct a

mutagenesis library. The binding modes of the GDHtR with ATP, CTP, or GTP, respectively, were simulated by semi-flexible docking, and little difference was discovered among these combination modes. This would be based on establishing quantitative structure-activity relationships between GDHtR and its ligands, and serve as a basis for finding out inexpensive ligands for replacement of ATP. The results and methods achieved in this study indicate their potential application in future enzymatic research and industrial production.

Acknowledgments This work was supported by the National Natural Science Foundation of China (No. 41176111 and No. 41306124), the State Key Program of the National Natural Science Foundation of China (No. 21336009), the Fundamental Research Funds for the Central Universities (No. 2013121029), the Foundation of South Oceanographic Research Center of China in Xiamen (No. 14GYY011NF11), and the Public Science and Technology Research Funds Projects of Ocean (No. 201505032-6).

Compliance with Ethical Standards

Conflict of Interest The authors state that they have no competing interests.

Authors' Contributions WJ designed and supervised the experiments and drafted this manuscript. WJL performed the binding modes and revised the manuscript. YH performed gene cloning and expression in *E. coli*, and revised the manuscript. SZW constructed a mutagenesis library and revised the manuscript. BSF conceived the study, designed and supervised the experiments, and is the corresponding author. All authors have read and approved the manuscript.

References

1. Doleyres, Y., Beck, P., Vollenweider, S., & Lacroix, C. (2005). Production of 3-hydroxypropionaldehyde using a two-step process with *Lactobacillus reuteri. Applied Microbiology and Biotechnology, 68*, 467–474.
2. Saxena, R. K., Anand, P., Saran, S., & Isar, J. (2009). Microbial production of 1,3-propanediol: recent developments and emerging opportunities. *Biotechnology Advances, 27*, 895–913.
3. Biebl, H., Menzel, K., Zeng, A.-P., & Deckwer, W.-D. (1999). Microbial production of 1, 3-propanediol. *Applied Microbiology and Biotechnology, 52*, 289–297.
4. Liao, D.-I., Dotson, G., Turner, I., Jr., Reiss, L., & Emptage, M. (2003). Crystal structure of substrate free form of glycerol dehydratase. *Journal of Inorganic Biochemistry, 93*, 84–91.
5. Yamanishi, M., Yunoki, M., Tobimatsu, T., Sato, H., Matsui, J., Dokiya, A., Iuchi, Y., Oe, K., Suto, K., & Shibata, N. (2002). The crystal structure of coenzyme B_{12}-dependent glycerol dehydratase in complex with cobalamin and propane-1, 2-diol. *European Journal of Biochemistry, 269*, 4484–4494.
6. Parikh, M. R., & Matsumura, I. (2005). Site-saturation mutagenesis is more efficient than DNA shuffling for the directed evolution of β-fucosidase from β-galactosidase. *Journal of Molecular Biology, 352*, 621–628.
7. Qi, X., Guo, Q., Wei, Y., Xu, H., & Huang, R. (2012). Enhancement of pH stability and activity of glycerol dehydratase from *Klebsiella pneumoniae* by rational design. *Biotechnology Letters, 34*, 339–346.
8. Qi, X., Sun, L., Luo, Z., Wu, J., Meng, X., Tang, Y., Wei, Y., & Huang, R. (2006). Rational design of glycerol dehydratase: swapping the genes encoding the subunits of glycerol dehydratase to improve enzymatic properties. *Chinese Science Bulletin, 51*, 2977–2985.
9. Toraya, T. (2002). Enzymatic radical catalysis: coenzyme B_{12}-dependent diol dehydratase. *Chemical Record, 2*, 352–366.
10. Kajiura, H., Mori, K., Tobimatsu, T., & Toraya, T. (2001). Characterization and mechanism of action of a reactivating factor for adenosylcobalamin-dependent glycerol dehydratase. *Journal of Biological Chemistry, 276*, 36514–36519.
11. Mori, K., & Toraya, T. (1999). Mechanism of reactivation of coenzyme B_{12}-dependent diol dehydratase by a molecular chaperone-like reactivating factor. *Biochemistry, 38*, 13170–13178.
12. Shibata, N., Mori, K., Hieda, N., Higuchi, Y., Yamanishi, M., & Toraya, T. (2005). Release of a damaged cofactor from a coenzyme B_{12}-dependent enzyme: X-ray structures of diol dehydratase-reactivating factor. *Structure, 13*, 1745–1754.

13. Yanping Zhang, Z. R., Chenyu, D., Li, C., & Cao, Z. (2004). Effect of ATP addition on 1, 3-propanediol biosynthesis from glycerol by *Klebsiella pneumoniae. The Chinese Journal of Process Engineering, 4*, 567–571.
14. Zhi Rao, Y. Z., Shen, J., Li, C., & Cao, Z. (2004). Effect of addition of ATP on cell growth and 1,3-propanediol production of *K. pneumoniae. Fine Chemical, 21*, 413–417.
15. Li, W.-J., Fang, B.-S., Hong, Y., Wang, X.-X., Lin, J.-X., & Liu, G.-L. (2006). Cloning and expression of the genes encoding glycerol dehydratase reactivase and identification of its biological activity. *Chinese Journal of Biotechnology, 22*, 950–955.
16. Liao, D.-I., Reiss, L., Turner, I., Jr., & Dotson, G. (2003). Structure of glycerol dehydratase reactivase: a new type of molecular chaperone. *Structure, 11*, 109–119.
17. Zhang, G. L., Xu, X. L., Li, C., & Ma, B. (2009). Cloning, expression and reactivating characterization of glycerol dehydratase reactivation factor from *Klebsiella pneumoniae* XJPD-Li. *World Journal of Microbiology and Biotechnology, 25*, 1947–1953.
18. Kuntz, I. D., Blaney, J. M., Oatley, S. J., Langridge, R., & Ferrin, T. E. (1982). A geometric approach to macromolecule-ligand interactions. *Journal of Molecular Biology, 161*, 269–288.
19. Calvaresi, M., Hoefinger, S., & Zerbetto, F. (2012). Probing the structure of lysozyme-carbon-nanotube hybrids with molecular dynamics. *Chemistry A European Journal, 18*, 4308–4313.
20. Guo, J., Li, J., Zhang, Y., Jin, X., Liu, H., & Yao, X. (2013). Exploring the influence of carbon nanoparticles on the formation of β-sheet-rich oligomers of $IAPP_{22\text{-}28}$peptide by molecular dynamics simulation. *PLoS One, 8*, e65579–e65579.
21. Kitjaruwankul, S., Boonamnaj, P., Fuklang, S., Supunyabut, C., & Sompornpisut, P. (2015). Shaping the water crevice to accommodate the voltage sensor in a down conformation: a molecular dynamics simulation study. *The Journal of Physical Chemistry B, 119*, 6516–6524.
22. Shen, J.-W., Wu, T., Wang, Q., & Kang, Y. (2008). Induced stepwise conformational change of human serum albumin on carbon nanotube surfaces. *Biomaterials, 29*, 3847–3855.
23. Shen, J.-W., Wu, T., Wang, Q., Kang, Y., & Chen, X. (2009). Adsorption of insulin peptide on charged single-walled carbon nanotubes: significant role of ordered water molecules. *ChemPhysChem, 10*, 1260.
24. Sun, X., Feng, Z., Hou, T., & Li, Y. (2014). Mechanism of graphene oxide as an enzyme inhibitor from molecular dynamics simulations. *ACS Applied Materials & Interfaces, 6*, 7153–7163.
25. Yang, L., & Gao, Y. Q. (2010). Effects of cosolvents on the hydration of carbon nanotubes. *Journal of the American Chemical Society, 132*, 842–848.
26. Zhang, L., Xiao, X., Yuan, Y., Guo, Y., Li, M., & Pu, X. (2015). Probing immobilization mechanism of alpha-chymotrypsin onto carbon nanotube in organic media by molecular dynamics simulation. *Science Reports, 5*, 9297–9297.
27. Zhiwei, F., Pearce, L. V., Xiaomeng, X., Xiaole, Y., Peng, Y., Blumberg, P. M., & Xiang-Qun, X. (2015). Structural insight into tetrameric hTRPV1 from homology modeling, molecular docking, molecular dynamics simulation, virtual screening, and bioassay validations. *Journal of Chemical Information and Modeling, 55*, 572.
28. Zuo, G., Huang, Q., Wei, G., Zhou, R., & Fang, H. (2010). Plugging into proteins: poisoning protein function by a hydrophobic nanoparticle. *ACS Nano, 4*, 7508–7514.
29. Padovani, D., Banerjee, R. and Klinman, J. P. (2009) A G-Protein Editor Gates Coenzyme B_{12} Loading and Is Corrupted in Methylmalonic Aciduria. *Proceedings of the National Academy of Sciences of the United States of America*, pp. 21567. National Academy of Sciences.
30. Daniel, R., Bobik, T. A., & Gottschalk, G. (1998). Biochemistry of coenzyme B_{12}-dependent glycerol and diol dehydratases and organization of the encoding genes. *FEMS Microbiology Review, 22*, 553–566.
31. Tobimatsu, T., Azuma, M., Matsubara, H., Takatori, H., Niida, T., Nishimoto, K., Satoh, H., Hayashi, R., & Toraya, T. (1996). Cloning, sequencing, and high level expression of the genes encoding adenosylcobalamin-dependent glycerol dehydrase of *Klebsiella pneumoniae. Journal of Biological Chemistry, 271*, 22352–22357.
32. (2002) pET System Manual (10th Edition). Merck Company, Germany.
33. TORAYA, T., & FUKUI, S. (1977). Immunochemical evidence for the difference between coenzyme-B_{12}-dependent diol dehydratase and glycerol dehydratase. *European Journal of Biochemistry, 76*, 285–289.
34. Toraya, T. (2000). Radical catalysis of B_{12} enzymes: structure, mechanism, inactivation, and reactivation of diol and glycerol dehydratases. *Cellular and Molecular Life Sciences, 57*, 106–127.
35. Brown, K. L., & Marques, H. M. (2005). Product stabilization in the enzymatic activation of coenzyme B_{12}: a molecular modeling study. *Journal of Molecular Structure: THEOCHEM, 714*, 209–215.
36. Dölker, N., Maseras, F., & Siegbahn, P. E. (2004). Stabilization of the adenosyl radical in coenzyme B_{12}-a theoretical study. *Chemical Physics Letters, 386*, 174–178.
37. Masuda, J., Shibata, N., Morimoto, Y., Toraya, T., & Yasuoka, N. (2000). How a protein generates a catalytic radical from coenzyme B_{12}: X-ray structure of a diol-dehydratase–adeninylpentylcobalamin complex. *Structure, 8*, 775–788.

38. Zhang, Z.-G., Yi, Z.-L., Pei, X.-Q., & Wu, Z.-L. (2010). Improving the thermostability of *Geobacillus stearothermophilus* xylanase XT6 by directed evolution and site-directed mutagenesis. *Bioresource Technology, 101*, 9272–9278.
39. Hattori, M. E. (2012). Molecular mechanism of ATP binding and ion channel activation in P2X receptors. *Nature, 485*, 207–212.
40. Honda, S., Toraya, T., & Fukui, S. (1980). In situ reactivation of glycerol-inactivated coenzyme B_{12}-dependent enzymes, glycerol dehydratase and diol dehydratase. *Journal of Bacteriology, 143*, 1458–1465.
41. Jiang, F., & Kim, S.-H. (1991). "Soft docking": matching of molecular surface cubes. *Journal of Molecular Biology, 219*, 79–102.
42. Garg, A. D., Krysko, D. V., Verfaillie, T., Kaczmarek, A., Ferreira, G. B., Marysael, T., Rubio, N., Firczuk, M., Mathieu, C., Roebroek, A. J. M., Annaert, W., Golab, J., de Witte, P., Vandenabeele, P., & Agostinis, P. (2012). A novel pathway combining calreticulin exposure and ATP secretion in immunogenic cancer cell death. *EMBO Journal, 31*, 1062–1079.
43. Giorgio, V., von Stockum, S., Antoniel, M., Fabbro, A., Fogolari, F., Forte, M., Glick, G. D., Petronilli, V., Zoratti, M., Szabó, I., Lippe, G., & Bernardi, P. (2013). Dimers of mitochondrial ATP synthase form the permeability transition pore. *Proceedings of the National Academy of Sciences of the United States of America, 110*, 5887–5892.
44. Jeongmin ChoiTanaka, K. C. Q. Q. L. Y. L. G. (2014). Identification of a plant receptor for extracellular ATP. *Science, 343*, 290–294.
45. Hargreaves, D. C., & Crabtree, G. R. (2011). ATP-dependent chromatin remodeling: genetics, genomics and mechanisms. *Cell Research, 21*, 396–420.